A BLG1 neural model implements the unique looming selectivity to diving target*

LUAN Hao[1], HUA Mu[2], ZHANG Yicheng[2,3], YUE Shigang[2], and FU Qinbing[2,4]**

1. School of Computer Science and Engineering, Tianjin University of Technology, Tianjin 300384, China

2. School of Computer Science, University of Lincoln, Lincoln LN6 7TS, UK

3. School of Automation, Guangdong University of Petrochemical Technology, Maoming 525000, China

4. School of Mathematics and Information Science, Guangzhou University, Guangzhou 510006, China

(Received 6 June 2022; Revised 18 July 2022)

The bistratified lobula giant type 1 (BLG1) neuron is an identified looming-sensitive neuron in crab's visual brain that demonstrates special sensitivity to diving targets, or descending approaching motions. In this paper, a novel neural model is proposed to shape such unique selectivity through incorporating a bio-plausible feedforward contrast inhibition synapse and a radially extending spatial enhancement distribution. Herein the synaptic connections and neuronal functions of this model are placed within a framework for matching and describing underlying biological findings. The systematic and comparative experiments have validated the proposed computational model that reconciles with the characteristics of BLG1 neurons in crab.

Document code: A **Article ID:** 1673-1905(2023)02-0112-5

DOI https://doi.org/10.1007/s11801-023-2095-0

Crabs are applicable animals for researching the neurophysiological bases of visual signal transferring and transmitting in arthropod visual systems, since they exhibit multiple-stage, and complex visually-guided behaviors[1]. Specially, a group of motion-sensitive neurons distributed on the lobula are thought to be the key in perceiving target motions and leading specific self-actions. These neurons are named as monostratified lobula giant type 1 and 2 (MLG1 and MLG2) neurons, bistratified lobula giant type 1 and 2 (BLG1 and BLG2) neurons[2]. The MLG1s and MLG2 neurons are assumed to be the central factors in continuously detecting and regulating the escaping direction and velocity when facing predators. Therefore, a lot of neuroanatomical and psychobiology studies have been made and tried to quantitative how the visual stimulus affect the neuronal responses. Based on the research findings, kinds of models have been proposed from neuronal dynamic aspect[3,4] and computer vision[5].

Although the underlying mechanism of BLG1 neuron is still unclear, the BLG1 responds to approaching motions earlier than MLGs, and appears sensitivity to stimulus elevation[2]. The crabs just categorize an approaching target as a prey and a predator based on the elevation information[2]. However, little has been done on modeling and mimicking the BLG1 neuron.

Here, we provide insight into modeling a neural model with motion perception enhancement for implementing the selectivity of BLG1 neurons to descending proximity of moving target, or diving target. The proposed model incorporates a bio-plausible feedforward contrast inhibition synapse and a spatial enhancement distribution.

Our previous computational model of MLG1s neuronal ensemble preliminarily mimics the crab's visual system[5]. Building upon the neuromophic architecture of the MLG1s model, herein we propose the BLG1 computational neural network with special selectivity of descending proximity. The proposed BLG1 neuromophic architecture is shown in Fig.1. Specially, a bio-plausible normalization mechanism and a feedforward contrast inhibition synapse have been introduced to accommodate the contrast invariance (N and C), and shaping the unique selectivity to diving target via the radially extending spatial enhancement distribution (K_{ae}). Taking inspiration from the latest studies of the *Drosophila* visual system[6-8], the basic function of the normalization-mechanism-based feedforward contrast inhibition synapse is that the visual interneuron compares the intensity with its neighbouring visual inputs, and compresses the visual signal in a fixed range to maintain input invariability. The formulation of the proposed neural model is elaborated as follows.

* This work has been supported by the National Natural Science Foundation of China (No.12031003), and the European Union's Horizon 2020 Research and Innovation Programme under the Marie Sklodowska-Curie Grant Agreement (No.778062 ULTRACEPT).

** E-mail: qifu@gzhu.edu.cn

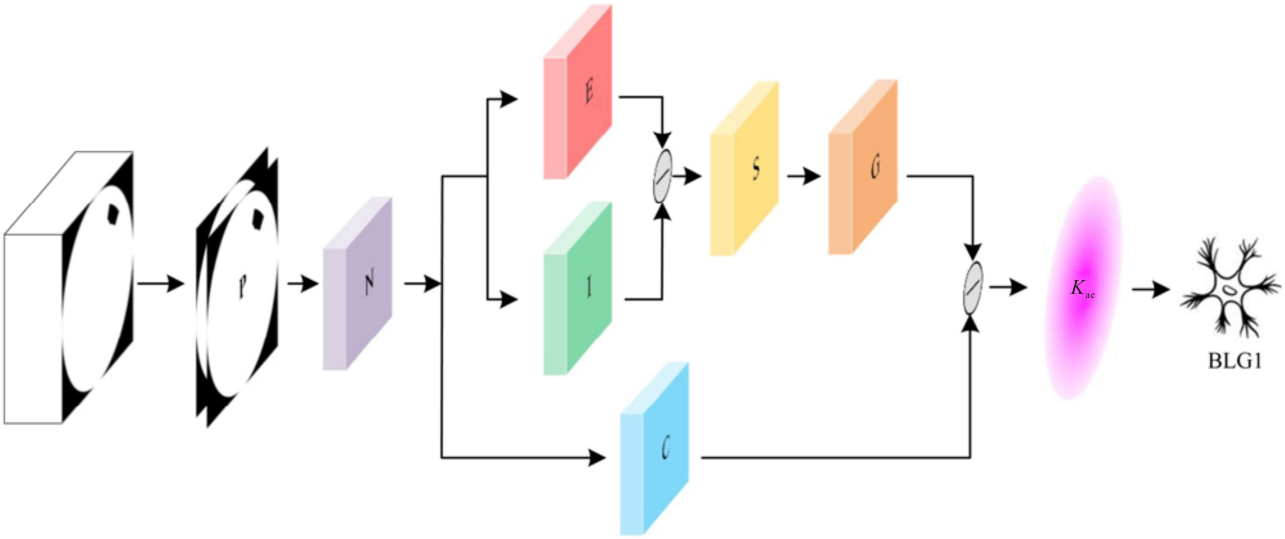

Fig.1 Neuromophic architecture of the proposed BLG1 neural network model (The proposed model utilizes the classic lateral-inhibition-mechanism-based feedforward neural network (P, E, I, S and G layers) and the novel normalization-mechanism-based (*N*) contrast inhibition synapse (*C*). Moreover, a radially extending spatial enhancement distribution (K_{ae}) characterizes the unique diving approaching motion selectivity.)

The photoreceptor layer mimics the function of the panoramic view of the crab, which computes the pixelwise luminance changes at successive frames.

$$\hat{P}(x,y,t) = | L(x,y,t) - \int L(x,y,t)\delta(t-s-1)\mathrm{d}s |, \quad (1)$$

where δ is the unit impulse function.

The principle of the bio-plausible normalization mechanism is comparing the luminance of center point with its neighboring local receptive fields, and transferring the compared value into a fixed range[7]. The calculation can be defined as follows

$$R(x,y,t) = \mathrm{Softsign}[\frac{\hat{P}(x,y,t)}{\alpha_1 + P(x,y,t)}], \quad (2)$$

where α_1 is luminance variance sensitivity of a local receptive field. The instantaneous parameter $P(x,y,t)$ is the center point value, which has been filtered by a classical Gaussian-kernel W_G with standard deviation σ_1.

$$P(x,y,t) = \iint \hat{P}(x,y,t) W_\mathrm{G}(x-u, y-v)\mathrm{d}u\mathrm{d}v, \quad (3)$$

$$W_\mathrm{G} = \frac{1}{2\pi\sigma_1^2}\exp(-\frac{u^2+v^2}{2\sigma_1^2}). \quad (4)$$

The separated excitation pathway and time-delayed inhibition pathway characterize the competition between local excitations and lateral inhibitions, which is a common feature in many crustaceans and insects[9]. The excitation pathway signal E equals the current normalized luminance change R, and the time-delayed inhibition pathway could be described as

$$I(x,y,t) = \iint R(x,y,t-1)\boldsymbol{W}_I(x-u, y-v)\mathrm{d}u\mathrm{d}v, \quad (5)$$

$$\boldsymbol{W}_I = -0.125 \times \begin{bmatrix} 1 & 2 & 1 \\ 2 & 0 & 2 \\ 1 & 2 & 1 \end{bmatrix}. \quad (6)$$

Subsequently, signals from excitation pathway and inhibition pathway are linearly integrated, and then filtered by a rectified linear unit (RELU) activation function. The summation S can be computationally presented as

$$S(x,y,t) = \mathrm{RELU}[E(x,y,t) + w_i \cdot I(x,y,t), 0]. \quad (7)$$

Mathematically speaking, the next grouping layer is a spatial filter to reduce isolated noises against cluttered scene. Specifically, C_e is the smoothed S via a mean filtering kernel, which is typically sized in a 3×3 matrix. The G layer calculations are as follows

$$C_\mathrm{e}(x,y,t) = \iint S(x,y,t) \cdot W_\mathrm{e}(x-u, y-v)\mathrm{d}u\mathrm{d}v, \quad (8)$$

$$\hat{G}(x,y,t) = S(x,y,t) \cdot C_\mathrm{e}(x,y,t) \cdot w^{-1}, \quad (9)$$

$$w = \Delta c + \max | C_\mathrm{e}(t) | \cdot C_w^{-1}, \quad (10)$$

where w is updated in real time, C_w is a constant coefficient, and Δc is a small real number.

Furthermore, the small excitation signals could be eliminated by a threshold T_g as

$$G(x,y,t) = \begin{cases} \hat{G}(x,y,t), & \text{if } \hat{G}(x,y,t) \geq T_\mathrm{g} \\ 0 & \text{otherwise} \end{cases}. \quad (11)$$

The mechanism of contrast inhibition synapse is achieved through the competition between the center point with peripheral surroundings.

The formulation of $\hat{C}$ is

$$\hat{C}(x,y,t) = R(x,y,t) - \iint R(x,y,t) W_\mathrm{C}(x-u, y-v)\mathrm{d}u\mathrm{d}v, \quad (12)$$

where W_C is the contrast inhibition kernel (see Fig.2), which can be defined as

$$W_\mathrm{C} = \lambda_1 \cdot \exp(-\frac{(x - v\cdot\cos\varphi)^2}{2\cdot\zeta^2}) \cdot \exp(-\frac{(y - v\cdot\sin\varphi)^2}{2\cdot\zeta^2}). \quad (13)$$

The current C is calculated by its previous value and the difference of two successive competitive values $\hat{C}$.

$$C(x,y,t) = \alpha_2 \cdot [C(x,y,t-1) + \hat{C}(x,y,t) - \hat{C}(x,y,t-1)], \quad (14)$$

$$\alpha_2 = \frac{\tau_1}{\tau_1 + \tau_i}, \tag{15}$$

where α_2 is a temporal smooth coefficient which depends on a time constant τ_1 and the temporal sampling interval τ_i.

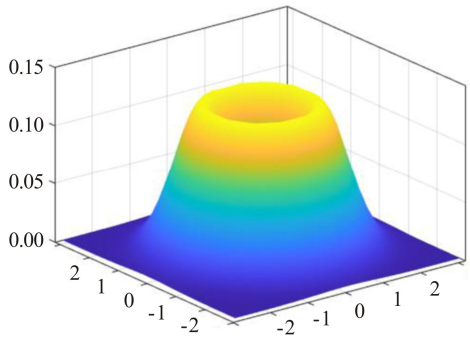

Fig.2 An example of the W_C kernel in 3D view, where λ_1=1, v=0.25, ζ=3

The motion excitation signal from the G layer and the contrast inhibition synaptic signal compete with each other, which can be defined as follows

$$C(x,y,t) = \begin{cases} C(x,y,t), & \text{if} \quad \hat{G}(x,y,t) \geq T_g \\ 0 & \text{otherwise} \end{cases}, \tag{16}$$

$$\hat{k}(x,y,t) = \text{RELU}[G(x,y,t) - \alpha_3 \cdot C(x,y,t), 0], \tag{17}$$

where $\hat{k}$ represents the motion cues in crab's panoramic view.

According to spatial distortion mapping of the panoramic receptive field, neuron signals in the central region represent the motion cues that happen in the sky area. Thus, we set a radially extending spatial enhancement distribution K_{ae}, to selectively enhance the signal generated by the descending approaching motions. The K_{ae} is shaped like a two-dimensional Gaussian kernel. The enhanced motion cues k and K_{ae} are formulated as follows

$$k(t) = \hat{k}(x,y,t) \cdot K_{ae}(x,y), \tag{18}$$

$$K_{ae}(x,y) = \beta_1 + \beta_2 \cdot \exp(-\lambda_2^2(x^2 + y^2)). \tag{19}$$

To integrate the motion cues, we use a rectifying operation to calculate the membrane potential MP, that is

$$MP(t) = \iint k(x,y,t)\text{d}x\text{d}y. \tag{20}$$

And NMP is the normalized MP by the Softsign function as

$$NMP(t) = \text{Softsign}(MP(t) \cdot n_{\text{cells}}^{-1}). \tag{21}$$

If the NMP continuously exceeds the spiking threshold, the BLG1 neuron could generate spikes, and the successive neuronal spikes indicate potential descending approaching event. The parameters of the proposed BLG1 neural model are listed in Tab.1.

Tab.1 Parameters setting

Name	Value	Name	Value	Name	Value
α_1	3	u, v	5	σ_1	5
w_i	0.3	C_w	4	Δc	0.01
T_g	0, 1.5	τ_1	140	α_3	1.5
T_s	0.45	n_{sp}	4		

Next, we systematically test and investigate the proposed neural model. Within this study, the experimental videos contain synthesized approaching stimuli within pure backgrounds and real nature background. The resolution of all experimental videos is 720×720 pixels, and the sampling rate is 60 fps. To verify the effectiveness and robustness of the contrast inhibition synapse, we set a group of test videos with different contrasts, of which we use the contrast evaluation ξ to estimate the contrast variance between the approaching target and background as

$$\xi = \left| \frac{I_{bg} - I_{obj}}{255} \right|. \tag{22}$$

It is worth pointing out that in the real-world scenario, the intensity of each local view field is not equal. Therefore, we only take the average intensity of the whole background to evaluate the contrast variance.

The first group of experiments is implemented to examine the effectiveness of the proposed feedforward contrast inhibition synapse. Note that the spatial enhancement distribution K_{ae} has been removed in this test.

In Fig.3(a), the background intensity in the first row is 0, and the intensities of approaching targets gradually decrease. Within the second row, the approaching target intensity is fixed to 255, and the background intensities increase by degrees. The contrast evaluation ξ is listed below the sub-figures. The comparative results in Fig.3(c) prove that in the pure normal backgrounds, the proposed neural model with contrast inhibition synapse could greatly reduce the contrast sensibility.

In Fig.3(b), the average intensity of such scenario is around 106, and the various contrast evaluations ξ in these experimental videos range from 0.02 to 0.56. The comparative model outputs shown in Fig.3(d) demonstrate the contrast inhibition synapse could improve the model's sensitivity for perceiving approaching event. Together, the systematic comparative results illustrate that the contrast inhibition synapse not only enhances the model's approaching event perceiving ability, but also reduces the variability of the neuronal membrane potential.

Furthermore, to investigate the unique selectivity of the proposed neural model to descending proximity differently to relevant models, characterized by the spatial enhancement distribution K_{ae}, we set an ablation experiment which respectively employs K_{ae} and the normalization-mechanism-based contrast inhibition synapse. The experimental videos contain a group of approaching motions from various altitudes. The videos are shown in Fig.4(a) and (b). Targets approaching from nine positions of the panoramic image are used to simulate the diving motions from diverse altitudes. The horizontal line has been set as position P=0 (see Fig.4(a)). The K_{ae} parameters for the neuronal comparative outputs shown in Fig.4(c) are β_1=1.2, β_2=1, λ_2=0.005. From the comparison of the neuronal responses, we can clearly see that the model couldn't perceive the approaching cues when the contrast inhibition synapse and K_{ae} are both not used (see red area). When implementing the K_{ae} only, the model couldn't produce reasonable response (pink area in

Fig.4(c)). The contrast inhibition synapse improves the sensibility of the model in detecting approaching motions, and the K_{ae} strengthened such ability proportionally in this test (blue area and green area, respectively).

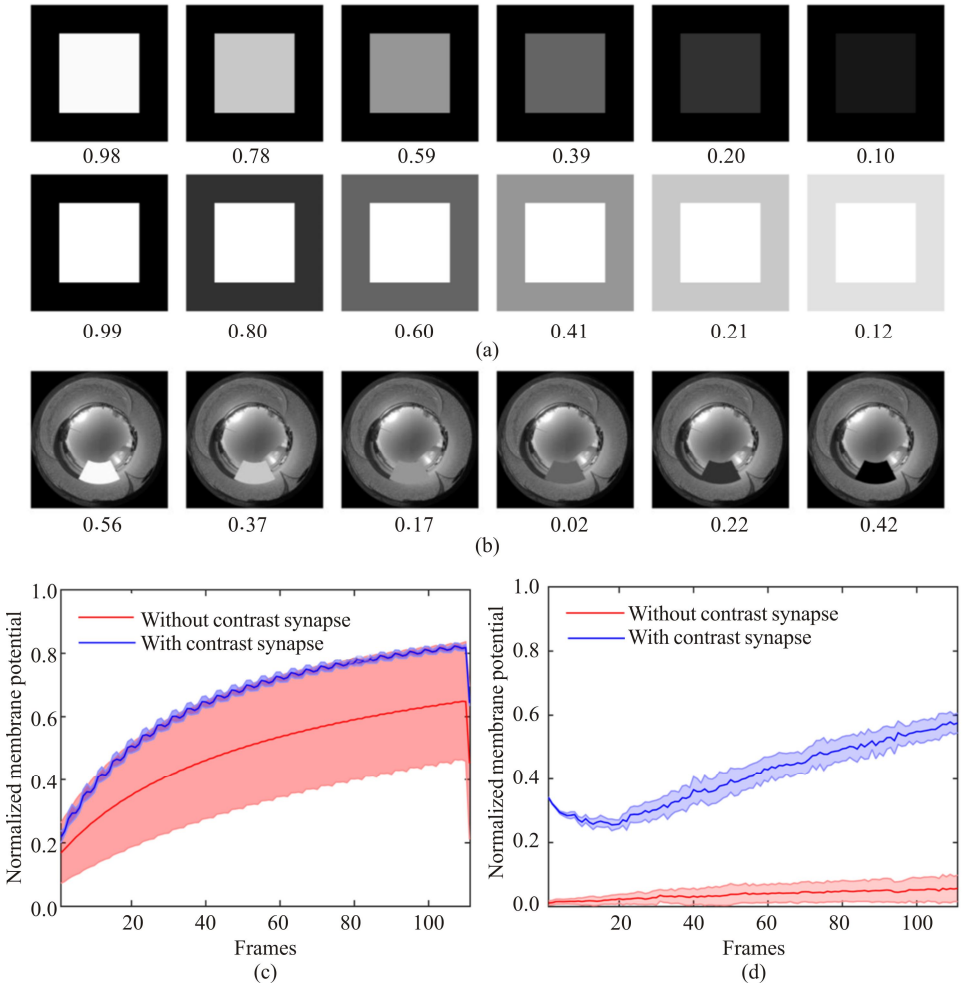

Fig.3 (a) A group of synthesized approaching videos in pure backgrounds (The number below each sub-figure is the contrast evaluation ξ. The background intensity of the first row is 0, and the approaching object intensity of the second row is 255); (b) A group of synthesized approaching videos in a panoramic nature view (The average intensity of the nature background is around 106); (c, d) Comparative results (shaded error area) of experimental videos respectively shown in (a) and (b) (The contrast inhibition kernel W_C is the same as shown in Fig.2)

The capacity in shaping the descending approaching selectivity of K_{ae} is shown in Fig.4(d). Within this test, the K_{ae} has been set as β_1=0, β_2=2, λ_2=0.005. The approaching motions happen below the horizontal line, and can't make the membrane potential exceed the spiking threshold, i.e., activate the BLG1 neuron (see the purple line and green line). When challenged by the approaching motion which begins around the horizontal line, the BLG1 neuron could hardly detect the approaching motions until the target is close enough (see yellow line in Fig.4(d)). Although in the panoramic image, the target at higher elevation will be spatially compressed smaller (comparing P=200 and P=100 in Fig.4(b)), the higher altitude approaching motion cues integrated and enhanced by K_{ae}, and promote the BLG1 neuronal membrane potential to exceed the spiking threshold earlier, i.e., the red membrane potential passes the threshold earlier than the blue line. Accordingly, the aforementioned experiments validate the proposed BLG1 neural model with robust performance against input variability on visual contrast and unique selectivity to diving target. The experimental results show that the proposed BLG1 model selectively responds to diving approaching motions.

In this paper, a novel neural model is proposed to implement the BLG1 neuron's selectivity in perceiving diving target via a spatial enhancement distribution K_{ae}. Meanwhile, a bio-plausible feedforward contrast inhibition synapse has been introduced to accommodate the contrast invariance of the model. The systematic and comparative experiments illustrate that our proposed BLG1 neural model not only perceives impending motions with more effectiveness and robustness, but also fits well with corresponding biological features, sensitive to motions

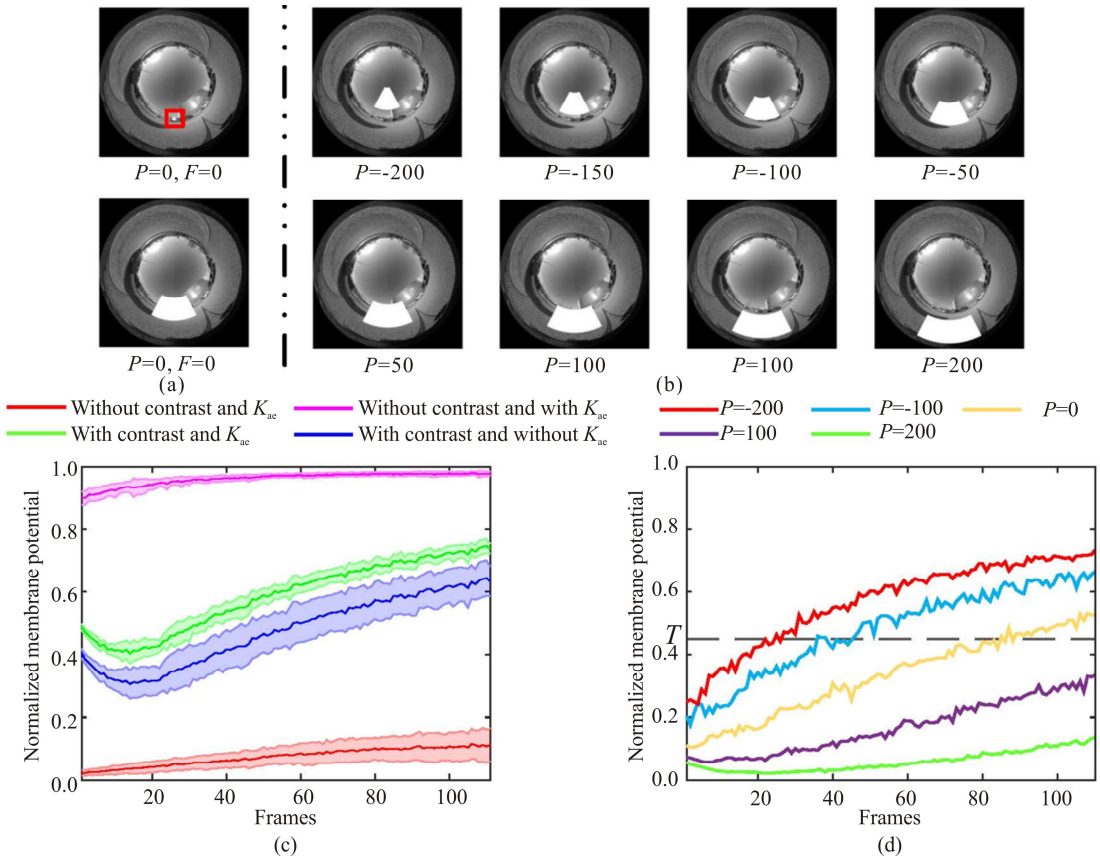

Fig.4 (a) An approaching target starts from the altitude of the horizontal line (The start point is marked as the red square. *F*=0 and *F*=100 represent the zero frame and the 100th frame, respectively); (b) A group of diving approaching motions from various altitudes (All subfigures are captured from the 100th frames of each video); (c) An ablation experiment illustrates the performance of the newly introduced normalization-mechanism-based contrast inhibition synapse and the spatial enhancement distribution K_{ae}; (d) A demonstration of the proposed model's selectivity to diving target (The dashed gray line indicates the spiking threshold *T*=0.45)

caused by diving target. In addition, some of the image pre-processing methods[10] could improve the performance of the photoceptor layer to extract moving targets more efficiently, which can also be involved in the present model.

Statements and Declarations

The authors declare that there are no conflicts of interest related to this article.

References

[1] CARBONE J, YABO A, OLIVA D. Characterization and modelling of looming-sensitive neurons in the crab Neohelice[J]. Journal of comparative physiology A, 2018, 204(5)：487-503.

[2] TOMSIC D, SZTARKER J, BERÓN DE ASTRADA M, et al. The predator and prey behaviors of crabs：from ecology to neural adaptations[J]. Journal of experimental biology, 2017, 220(13)：2318-2327.

[3] MEDAN V, DE ASTRADA M B, SCARANO F, et al. A network of visual motion-sensitive neurons for computing object position in an arthropod[J]. Journal of neuro science, 2015, 35(17)：6654-6666.

[4] OLIVA D, TOMSIC D. Computation of object approach by a system of visual motion-sensitive neurons in the crab Neohelice[J]. Journal of neurophysiology, 2014, 112(6)：1477-1490.

[5] LUAN H, FU Q, ZHANG Y, et al. A looming spatial localization neural network inspired by MLG1 neurons in the crab neohelice[J]. Frontiers in neuroscience, 2022, 15：787256.

[6] BAHL A, SERBE E, MEIER M, et al. Neural mechanisms for Drosophila contrast vision[J]. Neuron, 2015, 88(6)：1240-1252.

[7] DREWS M S, LEONHARDT A, PIROGOVA N, et al. Dynamic signal compression for robust motion vision in flies[J]. Current biology, 2020, 30：209-221.

[8] WIENECKE C F R, CLANDININ T R. Drosophila vision：an eye for change[J]. Current biology, 2020, 30(2)：R66-R68.

[9] RIND F C, BRAMWELL D I. Neural network based on the input organization of an identified neuron signaling impending collision[J]. Journal of neurophysiology, 1996, 75(3)：967-985.

[10] SUN P, LÜ L, QIN J. Moving object extraction based on saliency detection and adaptive background model[J]. Optoelectronics letters, 2020, 16(1)：59-64.